HEALTH AND MEDICINE

Perfusion, cryopreservation, and nanowarming of whole hearts using colloidally stable magnetic cryopreservation agent solutions

Andreina Chiu-Lam[1], Edward Staples[2], Carl J. Pepine[3], Carlos Rinaldi[1,4]*

Nanowarming of cryopreserved organs perfused with magnetic cryopreservation agents (mCPAs) could increase donor organ utilization by extending preservation time and avoiding damage caused by slow and nonuniform rewarming. Here, we report formulation of an mCPA containing superparamagnetic iron oxide nanoparticles (SPIONs) that are stable against aggregation in the cryopreservation agent VS55 before and after vitrification and nanowarming and that achieve high-temperature rise rates of up to 321°C/min under an alternating magnetic field. These SPIONs and mCPAs have low cytotoxicity against primary cardiomyocytes. We demonstrate successful perfusion of whole rat hearts with the mCPA and removal using Custodiol HTK solution, even after vitrification, cryostorage in liquid nitrogen for 1 week, and nanowarming under an alternating magnetic field. Quantification of SPIONs in the hearts using magnetic particle imaging demonstrates that the formulated mCPAs are suitable for perfusion, vitrification, and nanowarming of whole organs with minimal residual iron in tissues.

INTRODUCTION

Advances in transplantation technologies have contributed to improving the quality of life of patients affected by organ failure. On the basis of data from the Organ Procurement and Transplantation Network, in 2019, there were 39,718 transplants performed in the United States, but nearly 113,000 candidates remained on the waiting list. However, these numbers fail to capture the true magnitude of organ shortage worldwide. The World Health Organization estimated that in 2016 the number of solid organs transplanted (135,860) accounted for <10% of the actual need worldwide (*1*). This large gap between organ supply and demand suggests that the shortage of available organs is one of the greatest crises facing medicine today (*2*).

Since its inception, organ transplantation has saved millions of lives and improved the quality of life in many more. However, despite advances in surgery and organ preservation technologies, about 70% of organs suitable for transplant are discarded (*1*). One critical reason is exceeding preservation time limits in taking organs from donors to potential recipients (*3*). At present, the preservation time window ranges from 4 to 36 hours depending on the organ (*4*), severely restricting the time for adequate donor-to-recipient matching and the distance over which transplant organs can be offered. Time and distance restrictions result in a large number of organs that are not used while also contributing to using organs that are not ideally matched to recipients, based on size or immunological factors, for example. The latter situation contributes to patients requiring lifelong immunosuppressant drug regimens, adverse effects of which can increase the risk for life-threatening infections, cancer, and other diseases (*2*, *3*, *5*). Thus, technologies that enable biobanking of organs could revolutionize organ transplantation by "stopping the clock" on organ degradation. At the same time, in-depth donor-to-recipient matching is made possible, resulting in decreased recipient rejection and allowing treatment planning with reduced patient wait time (*3*).

The heart and lungs present some of the greatest challenges in organ transplantation, with approximately 70% of donated hearts and 80% of donated lungs going to waste (*2*). Regrettably, many of these discarded hearts could have been successfully transplanted if they could have been offered to areas outside the geographical range accessible in the first 1 to 2 hours of preservation (*2*). At present, hearts can only be preserved for up to 4 hours (*4*). Current organ preservation technologies involve flushing the organ with and immersion in a preservation solution before placing it on ice (*3*, *6*). The small organ preservation window limits the ability to match donor and recipient for immune markers adequately, makes coordination of organ harvesting and transplantation challenging, limits the geographical range accessible to match an organ to a recipient, adds to the cost burden of treating heart failure by transplantation, and results in loss of donated organs if the preservation window is exceeded.

One approach to biobanking of organs is cryopreservation by vitrification, where the organ is rapidly cooled to extremely low temperatures, below the glass transition, avoiding ice crystal formation and its associated damage to tissues (*7*). Vitrification relies on cryoprotecting agent (CPA) solutions that are perfused through the organ to prevent ice formation at practically feasible cooling rates (*7*). Cryopreservation by vitrification has successfully worked in small samples such as cells, ovaries, and embryos (*2*, *3*, *8*, *9*). Larger organs, such as rabbit kidneys (*10*) and rat hindlimb (*11*, *12*), have occasionally worked but have had a notable number of failures because of problems with achieving fast and uniform rewarming. As organs become larger, the chance of failure is greater due to devitrification and thermomechanical stress (*7*, *13*, *14*). These studies suggest that to translate biobanking by vitrification to whole organs successfully, one must overcome challenges associated with ice crystal formation and temperature gradients during rewarming (*3*, *7*). First, to avoid ice crystal formation due to devitrification during the rewarming step, one must achieve sufficiently fast heating rates (*7*, *15*). As an example, the commonly used cryopreservation solution VS55 has a critical cooling rate (CCR) of −2.5°C/min and a critical warming rate (CWR) of 50°C/min, illustrating the substantial

[1]Department of Chemical Engineering, University of Florida, Gainesville, FL 32611, USA. [2]Thoracic Surgery, University of Florida, Gainesville, FL 32611, USA. [3]Division of Cardiology, University of Florida, Gainesville, FL 32611, USA. [4]J. Crayton Pruitt Family Department of Biomedical Engineering, University of Florida, Gainesville, FL 32611, USA.
*Corresponding author. Email: carlos.rinaldi@ufl.edu

difference in cooling and heating rates required for typical CPA solutions for vitrification (*16*). CCR and CWR vary with cryopreservation agent formulation, and both decrease as the concentration of cryoprotectant agents increases. However, this results in increased chemical toxicity (*15*). Second, as the volume of the cryopreserved tissue increases, thermomechanical stress resulting from temperature gradients hinders organ survivability (*7*, *13*). Traditional rewarming approaches fail because heat must travel from the outside to the center of the organ, resulting in temperature gradients. These limitations suggest that technologies that achieve uniform, fast, controlled warming of cryopreserved organs are required to make cryopreservation by vitrification feasible for biobanking of whole organs.

One potential solution to the heat transfer challenges associated with the rewarming step is nanowarming (*14*). Nanowarming, introduced by Bischof and collaborators (*14*, *17*), is a volumetric heating approach where magnetic CPA (mCPA) solutions containing biocompatible superparamagnetic iron oxide nanoparticles (SPIONs) are used to vitrify a perfused organ or immersed tissue specimen (*3*). At the time of organ transplantation to a recipient, an alternating magnetic field (AMF) results in heat generation by the nanoparticles, rewarming the organ rapidly and uniformly. The AMF used penetrates the entire volume of tissue without attenuation, enabling uniform heating even in large organs (*18*). If the vitrified organ is uniformly perfused with the mCPA solution and nanoparticles are evenly distributed throughout the organ mass, the tissue will be rewarmed homogeneously, reducing thermomechanical stress. Furthermore, the temperature rise rate can be controlled by adjusting the concentration of nanoparticles in the mCPA, the magnetic properties of the nanoparticles, and the amplitude and frequency of the AMF used to actuate heat release.

There have been a few studies to date evaluating nanowarming of biologics. The first applied nanowarming to vitrified human mesenchymal cells (*19*), and the second applied nanowarming to vitrified fibroblasts, vessel segments, and heart valve leaflets (*17*). In both cases, cells and tissues were vitrified by immersion in an mCPA. In a more recent study, a silica-coated iron oxide nanoparticle was reported to have improved stability in the CPA VS55 (*20*). This study reported nanowarming of vitrified cells and perfusion of rat kidneys. However, the authors did not report cryopreservation by vitrification or nanowarming of whole organs. The application of magnetic resonance imaging to assess SPION distribution in hindlimbs, livers, kidneys, and ovaries perfused with mCPA was recently evaluated (*21*). In this study, the organs were perfused with mCPA and cryopreserved, but not nanowarmed using an AMF. Furthermore, the results suggest heterogeneous distribution of the SPIONs in the organs and the challenges with quantitative assessment of SPION distribution using magnetic resonance imaging at the nanoparticle concentrations typically required for nanowarming. While these key studies demonstrated that nanowarming is possible with negligible damage to cells and tissues, the immersion approach used is not suitable for whole organs, as the CPA solution and SPIONs will not distribute uniformly throughout the organ. To date, successful perfusion, vitrification, and nanowarming of a whole organ using an mCPA has not been reported. One possible contributor to this absence is the lack of SPION stability against aggregation in CPA solutions or aggregation during the vitrification or nanowarming steps, as has been previously acknowledged (*17*, *21*). CPA solutions contain high concentrations of dimethyl sulfoxide (DMSO), 1,2-propanediol, ethylene glycol, glycerol, salts, and other components that could impair nanoparticle colloidal stability. Furthermore, nanoparticle solutions risk irreversible aggregation when freezing unless stabilizing agents are used (*22*, *23*). Aggregation of nanoparticles in mCPA could hinder their penetration into microcapillaries, resulting in nonuniform organ distribution and nonuniform heating rates. Furthermore, aggregation could result in blocked blood vessels or prevent complete removal of nanoparticles from microcapillaries, which could result in organ damage due to restricted blood flow once transplanted.

Here, we report formulation of SPIONs coated with a dense, covalently grafted brush of polyethylene glycol (PEG) that are stable against aggregation in CPA solutions for prolonged periods and after vitrification and nanowarming from liquid nitrogen temperature to room temperature. We demonstrate that this mCPA has fast heating rates, controllable through the magnitude of the applied AMF and SPION composition. We further demonstrate that these mCPAs can uniformly perfuse whole rat hearts and be efficiently removed even after vitrification, cryostorage in liquid nitrogen for 1 week, and nanowarming to room temperature, without evidence of damage to the heart. For this purpose, we demonstrate the application of magnetic particle imaging (MPI) to quantitatively assess SPIO loading in the organ before and after vitrification and nanowarming. MPI quantifies the spatial three-dimensional (3D) distribution of iron oxide nanoparticle tracers (*24*, *25*). The image signal in each voxel is proportional to the concentration of the particles, and there is negligible signal attenuation by tissue. Together, these studies suggest the potential of the SPIONs and mCPA solutions reported here for whole-heart cryopreservation and nanowarming.

RESULTS

SPIONs that are stable in VS55 before and after vitrification and nanowarming

SPIONs were synthesized by the coprecipitation method. The size distribution of the iron oxide cores, obtained by transmission electron microscopy, was fitted to lognormal size distribution, resulting in a number-weighted mean core diameter of 12.6 nm and geometric deviation of 0.2 (fig. S1). The nanoparticles displayed superparamagnetic behavior (fig. S1), with small coercivity and remanence, and with a saturation magnetization of 82.4 Am^2/kg, close to the bulk value for magnetite of 86.6 Am^2/kg (*26*).

The colloidal stability of nanoparticles developed for biomedical applications is usually tested in saline solution or cell culture medium. Because of the complexity of cryopreservation solutions, which often contain high concentrations of DMSO and other chemicals, it is important to test the stability of nanoparticles in these solutions when formulating an mCPA. SPION ligand exchanged with PEGsilane [Monomethoxy polyethylene glycol conjugated with 3-aminopropyl triethoxysilane (APS)] using previously reported procedures (*27*) was purified with dialysis and magnetic separation to remove free PEGsilane. These nanoparticles were found to be unstable in VS55, aggregating quickly over a week (see fig. S2). We attributed these nanoparticles' poor colloidal stability in VS55 to unreacted amines resulting from remaining in PEGsilane (*27*). This results in a co-ligand exchange of PEGsilane and APTES APS. However, this also suggests that the resulting particles have primary amines on the surface that allow "backfilling" with additional PEG. This resulted in SPIONs with excellent colloidal stability in VS55, as observed in Fig. 1. SPIONs coated and

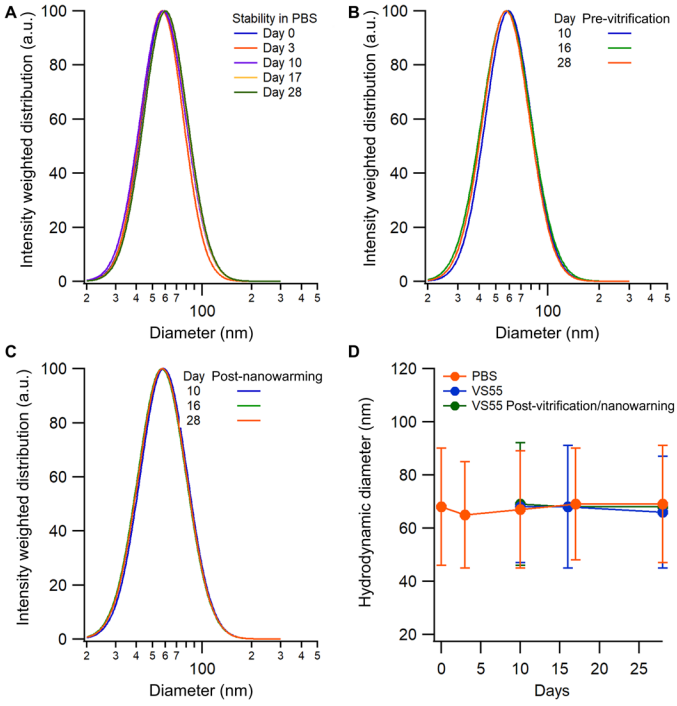

Fig. 1. Colloidally stable SPIONs consisting of a PEGsilane/APS coating backfilled with additional PEG. (**A**) Intensity weighted distribution of backfilled PEG-coated SPIONs in 1× PBS over 28 days. a.u., arbitrary units. (**B**) Intensity weighted distribution of backfilled PEG-coated SPIONs in VS55 (no vitrification). (**C**) Intensity weighted distribution of backfilled PEG-coated SPIONs in VS55 after vitrification and nanowarming. (**D**) Arithmetic mean and SD of the DLS hydrodynamic diameter for backfilled SPIONs in 1× PBS and VS55 before and after vitrification and nanowarming over 28 days.

backfilled with PEG were stable against aggregation in VS55 for 28 days. The next step was to verify that the nanoparticles remain stable in VS55 and after the sample is vitrified and nanowarmed in an AMF. SPIONs were suspended in VS55 for 10 days and then were vitrified and nanowarmed in an AMF. Stability was assessed immediately after nanowarming and periodically over the next 18 days. Figure 1C demonstrates that the particles are stable after vitrification. Figure 1D demonstrates that backfilled particles are the same size in phosphate-buffered saline (PBS) and VS55 before and after nanowarming and are stable against aggregation for at least 28 days.

mCPA solution with fast and controllable nanowarming rates

Nanowarming rates in an AMF were evaluated for CPA and mCPA (10 mg_{Fe}/ml) solutions and compared to those achievable by immersion in a water bath (Fig. 2A). Under AMF (42.5 kA/m, 278 kHz), the maximum heating rate achieved in a vitrified mCPA sample of 20 ml was 321°C/min, far surpassing the CWR for VS55 of 50°C/min (*14*). In contrast, a VS55 sample treated under the same conditions did not rewarm quickly. Similarly, vitrified mCPA and VS55 solutions placed in a warm water bath (37°C) did not rewarm quickly.

For mCPA at 10 mg_{Fe}/ml under an AMF, the solution heats up quickly and control of heating rate is desirable to avoid overshooting of target temperature during rewarming because chemical toxicity of cryopreservation agent solutions increases with temperature. We first achieved control of heating rate by adjusting the strength of the applied AMF. Figure 2B demonstrates that the heating rate can be altered by controlling field strength. By holding frequency constant and changing the current in the coil, the field strength is adjusted. The results demonstrate that as field strength decreased, the heating rate decreased.

Another method to control the heating rate is through the concentration of backfilled PEG-coated SPIONs present in the mCPA. The concentration was varied from 1 to 10 mg_{Fe}/ml. Figure 2C demonstrates that the heating rate decreases with decreasing concentration at a fixed AMF of 42.5 kA/m and 278 kHz. From the warming rates obtained at different concentrations, Fig. 2D shows that there is a linear relationship between the warming rate and SPION concentration. While these results show the potential to control heating rates through SPION concentration, they also suggest the importance of achieving uniform SPION loading throughout the organ to achieve uniform heating rates. This result underscores the need for methods to quantify SPION distribution in vitrified organs noninvasively.

mCPA solutions with low cardiomyocyte toxicity

The toxicity of SPIONs and VS55 was evaluated in vitro to determine whether the formulated mCPA is viable for future studies. Because the organ of interest was the heart, we evaluated cytotoxicity in primary cardiomyocytes. Primary cardiomyocytes were isolated from 2- to 3-day-old rat hearts. First, the toxicity of backfilled PEG-coated SPIONs was tested in the cells. Figure 3A shows the percentage of viable cells for each group from the image analysis of the Hoechst-Propidium Iodide stain. From the results, even at the highest SPION concentration tested of 10 mg_{Fe}/ml, SPIONs do not appear cytotoxic to the cells.

Next, we evaluated the cytotoxicity of VS55 on primary cardiomyocytes. Previous studies have found that VS55 is slightly toxic to human dermal fibroblasts (*17*), but toxicity to primary cardiomyocytes is not reported. We tested the cytotoxicity of VS55 at different concentrations by exchanging cell culture medium with a VS55/medium mixture. We also tested cytotoxicity when the concentration of VS55 was gradually increased in steps up to 100% VS55 and replaced with mCPA containing SPIONs to mimic typical CPA perfusion protocols (*17*, *28*, *29*). All experiments were performed on ice in a cold room at 4°C to provide a temperature-controlled environment and minimize the chemical toxicity of VS55. VS55 is composed of 3.1 M DMSO, which is toxic to cells, and chemical toxicity increases in a temperature-dependent manner (*15*). The results in Fig. 3B show that replacing medium directly with VS55/medium mixtures containing more than 50% VS55 results in substantial cytotoxicity toward primary cardiomyocytes. However, gradually increasing the concentration of VS55 to 100%, followed by replacement with mCPA, resulted in 74% primary cardiomyocyte viability.

Whole-heart perfusion with mCPA assessed using MPI

Past studies on nanowarming of biologics with mCPA that have been performed with mCPA have used cells or small sections of tissue submerged in mCPA solution (*17*, *19*, *20*) or have reported nonuniform distribution of SPIONs for organs (liver, kidney, and ovary) and hindlimbs perfused with mCPA (*21*). We demonstrate that the mCPA reported here can perfuse a whole rat heart and can be removed afterward. In this study, we first perfused the hearts and lungs together because of the difficulty in ligating small pulmonary arteries and veins in the rat without damaging the heart. This will be less of a problem for experiments with larger subjects.

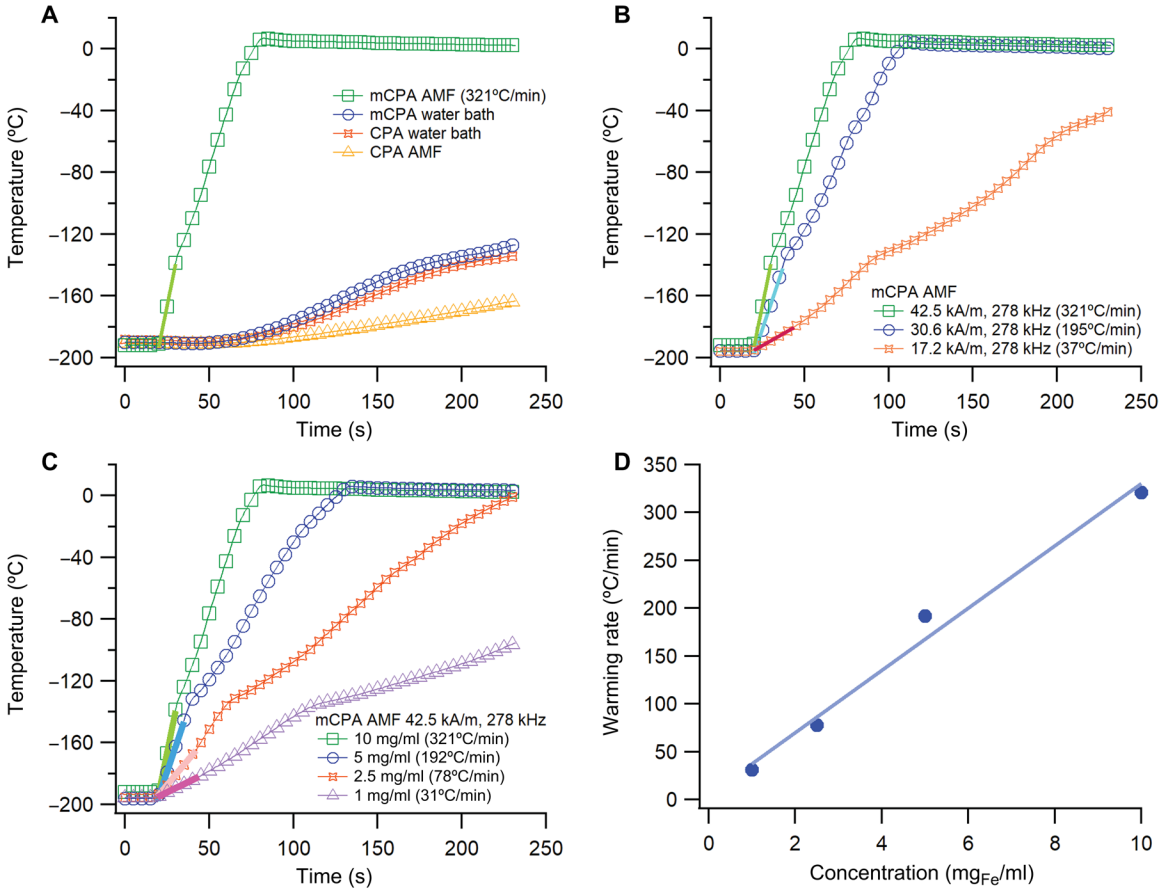

Fig. 2. mCPAs with exceptionally high and controllable heating rates. (**A**) Warming of CPA and mCPA solutions with SPION concentration of 10 mg_{Fe}/ml in a water bath at 37°C and AMF at 42.5 kA/m, 278 kHz. The nanowarming rate for mCPA in AMF is 321°C/min. (**B**) Nanowarming of mCPA (10 mg_{Fe}/ml) at different applied AMF conditions demonstrates control of the nanowarming rate. (**C**) Nanowarming rates at different SPION concentrations in VS55. Temperature profiles at different concentrations of SPIONs. (**D**) Relation between nanowarming rate and SPION concentration.

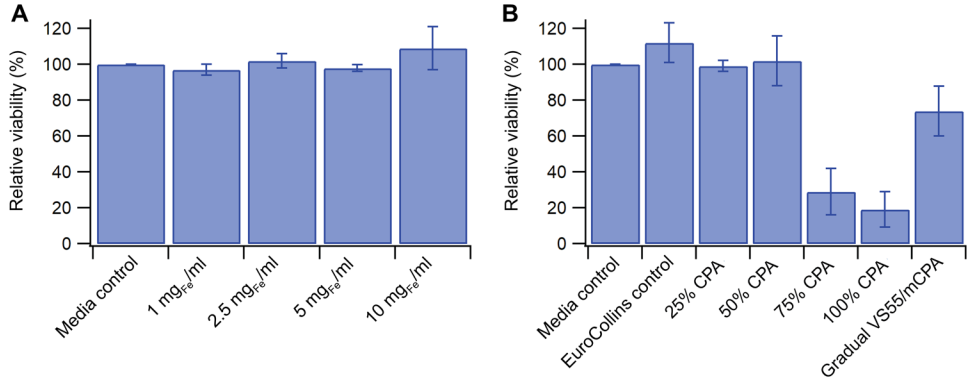

Fig. 3. SPIONs and mCPAs with low primary cardiomyocyte cytotoxicity. (**A**) Relative viability of primary cardiomyocytes incubated with PEG backfilled SPIONs. Viability reported as the percentage of live cells relative to total cells determined by Hoechst-PI. (**B**) Relative viability of primary cardiomyocytes incubated on ice for 1 hour with VS55/medium mixtures and after gradual addition of VS55 and replacement with mCPA. Relative viability reported as the percentage of live cells relative to total cells by Hoechst-PI.

To evaluate whether perfusion can be performed, the rat's heart and lungs were removed, perfused with Custodiol HTK first to remove the blood and arrest the heart, and then perfused with 100% mCPA. This was performed for three subjects to verify that the loading of particles was successful. Figure 4A is a representative photo of a heart perfused with mCPA, showing that the heart turns brown due to the uniformly distributed SPIONs. All three hearts were then removed from the lungs and placed in the MOMENTUM imager for quantitative imaging.

Once it was determined that the heart could be perfused with mCPA, the next step was to remove the mCPA. Using additional hearts perfused with mCPA, the mCPA was perfused out of the

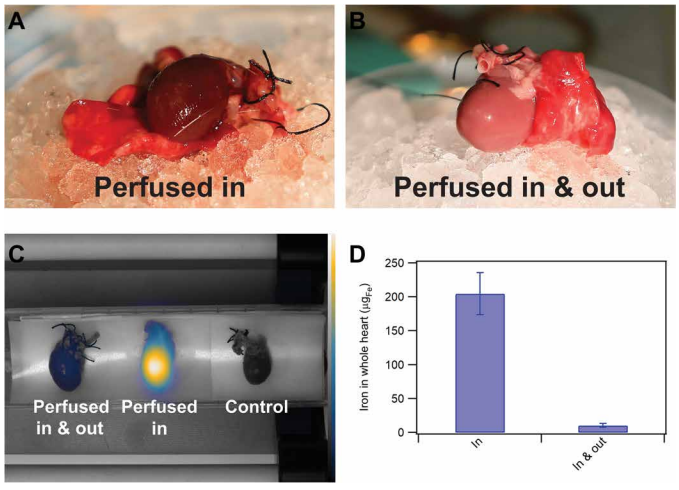

Fig. 4. Evaluation of heart perfusion with mCPA using MPI. (**A**) Representative photo of a heart well perfused with mCPA at 1 mg_{Fe}/ml. (**B**) Representative photo of a heart perfused in with mCPA at 1 mg_{Fe}/ml and then out with Custodiol HTK. (**C**) Co-registered image of hearts with their respective MPI signals, including (left to right) heart perfused in with mCPA and then out with Custodiol HTK, heart perfused in with mCPA, and control heart perfused with Custodiol HTK. (**D**) SPION iron mass in whole hearts determined from quantification of the MPI signal for $n = 3$ hearts perfused in and $n = 4$ hearts perfused in with mCPA and out with Custodiol HTK. Photo credit: Edward Staples, University of Florida.

heart using Custodiol HTK. Figure 4B is a representative photo of a heart after perfusing out the mCPA, showing that the heart color is now pink because most of the particles have been removed. This was performed in four hearts to verify that unloading of particles was reproducible. These hearts were then placed in a MOMENTUM imager for quantitative imaging.

Figure 4C is a representative co-registered image of one heart from each group and the signal from MPI. The co-registered image for the heart perfused in shows that the SPIONs were well distributed throughout the heart. The signal intensity of the particles from the MPI is proportional to the concentration of the particles. It can be observed from Fig. 4C that the heart perfused with mCPA shows a bright signal, whereas the heart perfused in and out shows a faint signal. There is no signal from the control heart. Individual MPI images for the hearts in each group can be found in the Supplementary Materials (fig. S3). These results show a 95% reduction in SPION mass from the hearts after perfusing out with Custodiol HTK, suggesting effective removal of the mCPA, as shown in Fig. 4D.

Histological analysis was performed for all hearts, and representative images of whole hearts from each group can be found in the Supplementary Materials (figs. S4 to S6). Hematoxylin and eosin (H&E) stains showed that the myocardium's cytoarchitecture is similar across groups, suggesting no gross macroscopic damage to the heart tissue. The use of Prussian blue, a complementary technique to visualize iron, further demonstrated that the SPIONs were perfused in and out of the heart. Cross sections of hearts perfused in with mCPA showed blue stains throughout the heart in the interstitial space, while the blue stain could no longer be observed in hearts perfused in and out.

Demonstration of whole-heart mCPA perfusion, vitrification, cryostorage, and nanowarming

Next, we evaluated whether mCPA can be perfused out after heart vitrification, cryostorage, and nanowarming. Figure 5 illustrates the procedure for these experiments. Figure 6A is an example of a heart successfully perfused with mCPA, vitrified to liquid nitrogen temperature, cryostored in liquid nitrogen for 1 week, nanowarmed in an AMF, and perfused out with Custodiol HTK. The heart looks intact visually, and the mCPA was successfully removed after nanowarming with Custodiol HTK, as indicated by the uniform pink color of the heart. Using MPI, it was determined that about 90% of the SPIONs were removed.

While Fig. 6A demonstrates successful mCPA perfusion and removal after vitrification, cryostorage, and nanowarming, we note that there were also several failed attempts at perfusing and removing the mCPA, some of which are represented in Fig. 6B. Examples of reasons for failure to perfuse in or out with mCPA included problems with air bubbles being entrained during perfusion, cracking of the heart during the nanowarming step, and problems caused by not fully submerging the heart in mCPA solution before vitrification. While these failed attempts underscore the need for further technique development, the results of Fig. 6A show the potential to uniformly perfuse hearts with mCPA and then remove the SPIONs after vitrification, biobanking at liquid nitrogen temperature, and nanowarming.

As noted previously, it is critical to uniformly perfuse the organ with mCPA and achieve uniform SPION distribution to obtain uniform heating during the nanowarming step. As such, techniques that allow noninvasive quantitative evaluation of SPION distribution in the heart are of great interest. MPI can be used to quantify and assess the distribution of SPIONs in hearts. This is illustrated in Fig. 6C, which shows optical and MPI images of a heart that was well perfused with mCPA and a heart that was poorly perfused due to obstruction of the right ventricle with an air bubble. Because MPI can provide a 3D quantitative and tomographic view of the distribution of SPIONs in whole organs, these results suggest the potential of MPI for evaluation of successful mCPA perfusion before vitrification. Furthermore, MPI could be coupled with the ability to control the location of SPION heating (*30*), which would enable control of the resulting temperature distribution during nanowarming.

DISCUSSION

The promise of nanowarming for biobanking of whole organs rests on the ability to uniformly perfuse an organ, vitrify the organ, and rapidly rewarm the organ to room temperature, avoiding damage caused during the rewarming step. It also requires removal of the SPIONs used to rewarm the organ. In this study, we demonstrated that SPIONs especially formulated for exceptional stability in the cryopreservation agent VS55 result in an mCPA that can uniformly perfuse whole rat hearts. We further demonstrated that whole rat hearts could be vitrified after perfusion with this mCPA, cryostored in liquid nitrogen for 1 week, and rapidly nanowarmed to room temperature with no evidence of macroscopic damage after vitrification, cryostorage, and nanowarming. These results highlight the important role of SPION stability in formulating mCPA solutions and support the potential of nanowarming as a strategy for biobanking transplant tissues.

Particles coated for biomedical applications are usually tested for stability in saline solution and medium only. However, because of the complexity of cryopreservation solutions, which often contain high concentrations of DMSO and other chemicals, it is important to test the particles' stability when formulating an mCPA. To date,

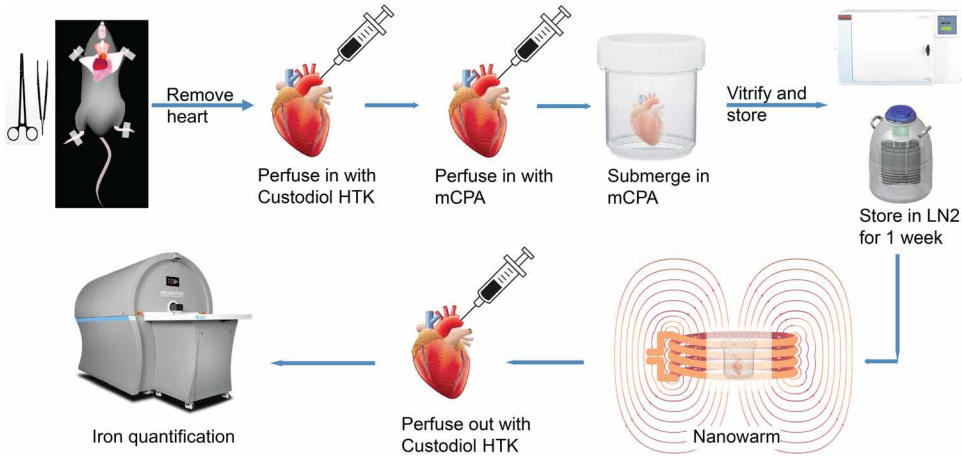

Fig. 5. Procedure for the ex vivo evaluation of mCPA perfusion and removal after vitrification and nanowarming. Hearts were removed from male rats and perfused with Custodiol HTK solution. Then, the heart was perfused with mCPA containing 5 mg_{Fe}/ml. The perfused heart was submerged in mCPA and vitrified in a mechanical freezer at a cooling rate of 15°C/min, followed by storage in liquid nitrogen for 1 week. Nanowarming was performed in an AMF (42.5 kA/m and 278 kHz, achieving heating rates above the CWR of 50°C/min for VS55. The SPIONs were perfused out of the heart using Custodiol HTK, followed by MPI to quantify the SPIONs remaining in the hearts. LN2, liquid nitrogen.

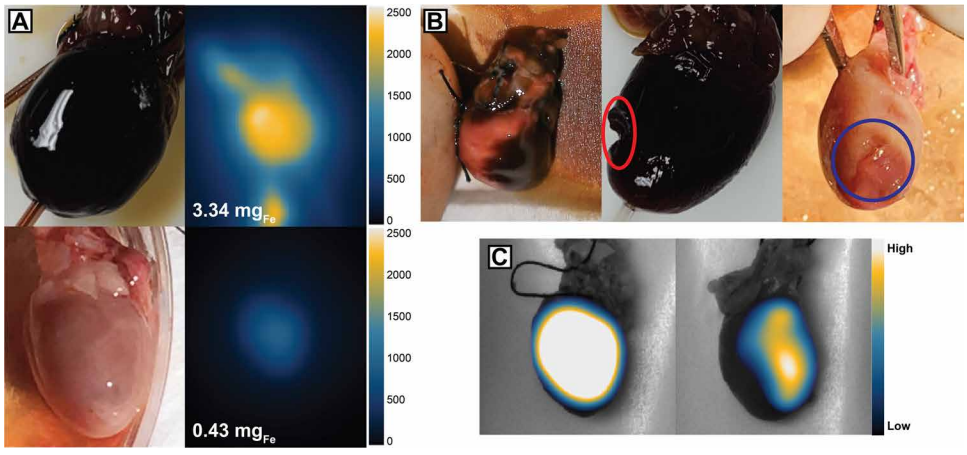

Fig. 6. Evaluation of mCPA perfusion, vitrification, cryostorage, and nanowarming of whole rat hearts. (**A**) Example of successful perfusion with mCPA, vitrification to 77 K, cryostorage at 77 K for 1 week, nanowarming with AMF (42.5 kA/m, 278 kHz), and subsequent removal of mCPA with Custodiol HTK. Optical and MPI images after perfusion with mCPA, vitrification, cryostorage, and nanowarming (top) and after removal of mCPA (bottom). Iron mass in the heart was determined using MPI. (**B**) Examples of failed attempts. Left: Example of nonuniform perfusion of mCPA due to obstruction of the right ventricle. Middle: Example of heart damage (red oval) due to rewarming using external heating (not nanowarming). Right: Example of heart damage (blue circle) due to nonuniform nanowarming caused by the heart not being completely immersed in mCPA. The heart did not perfuse well as observed from the color difference at the bottom of the heart compared to the top of the heart. (**C**) Use of MPI to distinguish uniform (left) and nonuniform (right) perfusion with mCPA. The heart shown in the right of (C) is the same as the heart shown in the left of (B), which had an obstruction in the right ventricle. Photo credit: Edward Staples and Andreina Chiu Lam, University of Florida.

the stability of SPIONs in CPA had not been demonstrated, despite its importance for storage before use and for successful whole-organ perfusion. Here, we have demonstrated that particles coated with PEG are initially not colloidally stable in VS55. However, once backfilled with more PEG, SPIONs were stable in VS55 for at least 1 month.

Nanoparticle solutions often risk irreversible aggregation when freezing unless stabilizing agents are used (*22*, *23*). Here, we demonstrated the stability of SPIONs in CPA after vitrification and rewarming without stabilizing agents, as these can affect the behavior of CPAs. The backfilled PEG-coated SPIONs in VS55 were stable for at least a month in VS55, and the particles were the same size as in PBS after nanowarming, indicating that no aggregation occurred. These results suggest that the formulated mCPA is stable and can potentially perfuse in and out of whole organs after vitrification and rewarming.

Nanowarming is only effective for cryopreservation if the CWR of the cryopreservation agent can be achieved volumetrically. The formulated mCPA consisting of stable SPIONs in VS55 achieved an exceptionally high-temperature rise rate of up to 321°C/min under an AMF with an amplitude of 42.5 kA/m and a frequency of 278 kHz, far exceeding the required CWR of VS55 (50°C/min). The temperature rise was controllable by altering the field amplitude or changing the nanoparticles' concentration in VS55. Furthermore, this suggests that the SPIONs reported here could be used to formulate cryopreservation solutions with lower chemical toxicity but concomitant higher CWR requirements, such as DP6, which requires a minimum heating rate of 185°C/min (*17*).

Loading of both CPA and SPIONs into whole organs with minimal toxicity is required for biobanking by vitrification to be translatable. As a first step, we evaluated the cytotoxicity of VS55 and the formulated mCPA in vitro. Cardiomyocytes loaded directly with SPIONs at up to 10 mg_{Fe}/ml had no change in viability. In 1999, Taylor *et al.* (*28*) introduced a multistep protocol for loading and unloading CPA as a way to reduce toxicity from CPA solutions. The literature shows that VS55 can be loaded into tissues and organs with reduced toxicity using multistep protocols at low temperatures (*10*, *15*, *28*, *29*, *31*). Osmotic effects are reduced by this stepwise increase in cryoprotective agent concentration, while the rapid transfer and low-temperature help prevent damage by chemical toxicity. Following this multistep protocol with the addition of SPIONs at the end of VS55 loading, negligible toxicity was observed in the cardiomyocytes (Fig. 4), compared to not using the multistep protocol.

Last, the ability to perfuse in and out of whole organs was demonstrated using the biomedical imaging technology MPI in whole hearts from rats. We demonstrated, through photography, MPI, and histology, that we can perfuse whole rat hearts with mCPA and perfuse out at least 95% of all SPIONs that were perfused into whole rat hearts (Fig. 6). In our studies, the amount of iron remaining after removal of SPIONs was 10.2 ± 2.7 μg_{Fe}. If transplanted to another rat, this would correspond to approximately 0.034 μgFe kg^{-1} body weight based on 300 g of body weight. Uncoated iron oxide nanoparticles have a reported limiting dose (LD-50) of 300 to 600 mg_{Fe} kg^{-1} body weight in rodents, and polysaccharide-coated particles have been shown to have a much higher LD-50 of 2000 to 6000 mg_{Fe} kg^{-1} (*32*). Furthermore, the bioconversion of iron oxide nanoparticles to iron in hemoglobin and ferritin is well documented, suggesting that the risk of toxicity due to residual SPIONs in the transplanted heart will be low (*32*). It is also important to assess and quantify the distribution of the nanoparticles in the heart to determine that uniform nanowarming can be achieved. Using MPI, we were able to quantify SPION loading and removal in whole rat hearts and assess mCPA distribution throughout the heart, comparing cases with successful and unsuccessful perfusion (Figs. 5 and 6). Further, we demonstrated successful whole-heart perfusion with mCPA, vitrification to liquid nitrogen temperature, cryostorage in liquid nitrogen for 1 week, nanowarming in AMF, and removal of SPIONs and illustrated examples of unsuccessful perfusion that suggest improvements needed to achieve uniform mCPA perfusion and nanowarming.

The mCPA solutions reported here, consisting of SPIONs especially formulated to be colloidally stable in the cryopreservation agent VS55, have low toxicity to primary cardiomyocytes, can achieve exceptionally high heating rates from liquid nitrogen temperature to room temperature, and can uniformly perfuse and be removed from whole hearts. We successfully demonstrate whole-heart perfusion, vitrification to liquid nitrogen temperature, cryostorage in liquid nitrogen for 1 week, nanowarming in an AMF from liquid nitrogen temperature to room temperature, and removal of the iron oxide nanoparticles through a combination of optical imaging and MPI. These studies support the potential of nanowarming using mCPA solutions to change current organ preservation paradigms and greatly enhance the availability of viable donor organs for transplantation. Future studies must address limitations by exploring perfusion process conditions, such as applying a gradual stepwise increase in mCPA concentration during the perfusion stage and assessing vascular tissue damage following vitrification and nanowarming. Furthermore, because of the high heating rates possible with the formulated mCPA, future studies could evaluate their use with CPA formulations with reduced chemical toxicity, as the concomitant larger CWR requirements may be met. Last, it will be important to test the ability of these mCPA formulations in achieving uniform perfusion of other organs and vascularized composite allografts.

MATERIALS AND METHODS

SPION synthesis

SPIONs were synthesized by a coprecipitation method optimized to produce particles with high-energy dissipation rates, described by others (*33*). Deionized water was deoxygenated for 30 min by bubbling nitrogen. Then, 3.98 g of iron(II) chloride tetrahydrate (99%; Sigma-Aldrich) and 10.81 g of iron(III) chloride hexahydrate (99%; Sigma-Aldrich) were dissolved in 100 ml of the deoxygenated deionized water. Once the iron salt solutions are dissolved, each solution was deoxygenated for 5 min and mixed in a glass reactor. The reaction mixture was heated to 75°C, and approximately 35 ml of ammonium hydroxide [29% (v/v), Thermo Fisher Scientific] was quickly added to the mixture (the pH should have reached 8.0 to 8.5). The reaction temperature was then increased to 85°C. The synthesis was conducted for 1 hour while maintaining a pH of around 8.0 to 8.5 by periodic addition of ammonium hydroxide. The resulting SPIONs were centrifuged, and the supernatant was discarded.

The black colloid from synthesis was suspended in tetramethylammonium hydroxide (TMAOH; 1 M; Sigma-Aldrich) at a volume ratio of 1:2 SPION/TMAOH. The peptization process was performed twice using an ultrasonicator (Q700, Qsonica Sonicators) for 30 min each time. The suspension was centrifuged again, and the peptized SPIONs were resuspended in water.

Oleic acid (OA; 90%; Sigma-Aldrich) adsorption onto the nanoparticles is required to coat the SPIONs with PEG. OA/g SPION (15 g) was added to the SPION solution and ultrasonicated (Q700, Qsonica Sonicators) for 15 min. The mixture was transferred to a glass reactor, where it was heated to 50°C and held at temperature to react for 2 hours. Precipitation of the SPIONs was performed using twice the volume of ethanol (200 proof, Decon Laboratories) and magnetically decanted to separate the particles, which were finally suspended in toluene (>98%; Sigma-Aldrich).

SPION coating with PEG

A two-step process was used to synthesize PEGsilane. First, 5-kDa molecular weight monomethoxy PEG (mPEG; 99.999%; Sigma-Aldrich) was converted to mPEG-COOH as described by Lele and Kulkarni (*34*). Briefly, 50 g of mPEG was dissolved in 400 ml of acetone (99.8%; Fisher Chemicals). Jones reagent, a strong oxidizing agent composed of chromium trioxide in aqueous sulfuric acid, was used to oxidize mPEG. Once the mPEG was dissolved in acetone, 16.1 ml of Jones reagent was added and reacted for 24 hours. Excess isopropyl alcohol (70%; Sigma-Aldrich) was added to stop the reaction. Activated charcoal (12 to 40 mesh, ACROS Organics) was used to remove impurities from the reaction. Activated charcoal and chromium salts were removed by vacuum filtration. Then, the acetone solution containing the oxidized mPEG was concentrated using a rotary evaporator. The concentrated mixture of mPEG-COOH was redissolved in 1 M hydrochloric acid [37% (w/v); Fisher Chemicals]. The polymer was extracted to the organic phase by liquid-liquid

extraction using approximately 75 to 100 ml of dichloromethane (>99.5%; Sigma-Aldrich). The process was performed twice, and all of the solution was concentrated by rotary evaporation. Last, mPEG-COOH was precipitated using cold diethyl ether (>99.8%; Fisher Chemicals). mPEG-COOH was then dried in a vacuum oven at room temperature.

PEGsilane was obtained by performing amidation of mPEG-COOH with APS (TCI America). Briefly, mPEG-COOH was weighed and melted in an oil bath set to 60°C. Then, APS was added to the melted PEG at a 1:1 molar ratio of mPEG-COOH/APS. The mixture was allowed to react for 2 hours at 120°C and 500 mbar. PEGsilane was then cooled to room temperature and hardened.

The SPIONs were coated with PEGsilane using ligand exchange, replacing the OA on the surface of the nanoparticles with PEGsilane, following a previously described procedure (*27*). Briefly, 3.5 g of PEGsilane was dissolved in 250 ml of dry toluene. A 45°C water bath was used to dissolve PEGsilane in toluene, and when dissolved, 250 ml of OA adsorbed SPIONs at 0.8 mg/ml and 40 μl of acetic acid (99.8%; ACROS Organics) were added and mixed. Acetic acid was used to catalyze hydrolysis and condensation of siloxane groups onto the SPION surface. The solution was then placed in a shaker for 72 hours. Cold diethyl ether was added to precipitate the nanoparticles to recover the PEGsilane-coated SPIONs. The precipitate was then dried in a vacuum oven at room temperature overnight. The next day, PEGsilane-coated SPIONs were resuspended in water and dialyzed to remove excess PEGsilane. For further purification, particles were purified using magnetic columns (Miltenyi Biotec).

Particles were stabilized by backfilling them with additional oxidized PEG using 1-ethyl-3-(3-dimethylaminopropyl)carbodiimide–*N*-hydroxysuccinimide (EDC-NHS) chemistry. The number of remaining primary amines on the particles was quantified using a CBQCA assay kit (Thermo Fisher Scientific), following the manufacturer's protocol. Once the number of amines was determined, a ratio of 1:10 amine to carboxylic acid was used. mPEG-COOH was suspended in water, and pH was adjusted to 5.0. A 1:2 ratio of carboxylic to EDC (Thermo Fisher Scientific) was added and allowed to react for 15 min to activate the carboxylic group. Then, sulfo-NHS (Thermo Fisher Scientific) was added at a 1:1 ratio of EDC to sulfo-NHS. The pH of the solution was slowly adjusted to 8.0, and the solution of particles was added once the pH was reached. The mixture reacted overnight and was then purified using a magnetic column as described above.

mCPA formulation

VS55 is an 8.4 M cryopreservation solution consisting of 2.2 M propylene glycol (Fisher Chemicals), 3.1 M formamide (Fisher BioReagents), 3.1 M DMSO (Fisher BioReagents), and 10 mM N-(2-Hydroxyethyl)piperazine-N′-(2-ethanesulfonic acid) (HEPES) (Fisher BioReagents) in Euro-Collins solution (*16*, *29*). Euro-Collins is composed of 194 mM D-glucose (Fisher BioReagents), 15 mM potassium phosphate monobasic (Fisher BioReagents), 42 mM potassium phosphate dibasic (Fisher BioReagents), 15 mM potassium chloride (Fisher BioReagents), and 10 mM sodium bicarbonate (Sigma-Aldrich) (*29*). Two hundred milliliters of a 5× concentrated Euro-Collins solution was mixed with 2.39 g of HEPES, 139.56 g of formamide, and 168.38 g of propylene glycol to make 1 liter of VS55. The solution was mixed well before adding 242.14 g of DMSO. Last, deionized water was added to complete to 1 liter. It was filtered through a 0.2-μm nylon filter before any in vitro or ex vivo experiments to sterilize the solution.

A stock solution of mCPA containing 10 mg_{Fe}/ml was produced by following the VS55 preparation procedure, but instead of adding deionized water at the end to complete to 1 liter, a solution of stable PEG-coated SPIONs suspended in deionized water at a concentration of 35 mg_{Fe}/ml was added. The solution was sterilized by filtering through a 0.2-μm nylon filter before any in vitro or ex vivo experiments.

Characterization of VS55, SPIONs, and mCPA

Dynamic light scattering

The hydrodynamic diameter of the particles was obtained by dynamic light scattering (DLS) using Brookhaven Instruments 90Plus/BI-MAS operating at room temperature. All measurements were made at a scattering angle of 90°.

Transmission electron microscopy

Samples were prepared for transmission electron microscopy (TEM) by depositing a drop of the nanoparticles in solution at 1 mg/ml on a formvar-coated copper grid. A JEOL 200CX microscope operated at 120 kV (Peabody, MA, USA) was used to obtain images. The number-weighted mean diameter and the geometric deviation were obtained by fitting the data to a lognormal size distribution.

Magnetic measurements

Equilibrium magnetic measurements were performed using a Quantum Design MPMS-3 Superconducting Quantum Interference Device (SQUID) magnetometer. Magnetization curves were obtained for dry SPIONs or 20 μl of mCPA at 10 mg_{Fe}/ml samples at 77.15 K in a magnetic field range of 7 to −7 T. From these curves, the experimental remanence and coercivity was determined.

Evaluation of nanowarming

Nanowarming of the mCPA solution was evaluated using 20 ml of solution in a 32-mm-diameter specimen jar. A fiber-optic temperature probe (Qualitrol) was placed in the middle of the sample to record the temperature. The sample was vitrified using a mechanical freezer by setting the freezer to cool at 15°C/min. Heating was performed by applying an AMF using an Ambrell EasyHeat induction heater. A control solution of VS55 was compared with an mCPA solution at 10 mg_{Fe}/ml to assess nanowarming. The warming of both solutions was evaluated by immersion in a water bath set at 37°C and separately by applying AMFs (42.5 kA/m peak, 278 kHz). The field amplitude and concentration of particles were varied separately to evaluate the control of nanowarming. The field strengths tested were 42.5, 30.6, and 17.2 kA/m peak at a frequency of 278 kHz. The concentrations used were 10, 5, 2.5, and 1 mg_{Fe}/ml.

SPION colloidal stability

Colloidal stability was assessed using DLS. SPIONs were suspended in 1× PBS or VS55 at approximately 0.5 mg_{Fe}/ml. Colloidal stability was assessed for a month. Stability before vitrification and after vitrification/nanowarming was assessed. A stock of 20 ml of mCPA at 10 mg_{Fe}/ml sample was made; at day 10, a 100-μl aliquot from the mCPA was obtained and diluted into 2 ml of VS55 for DLS measurements. The sample was then vitrified and nanowarmed. Once the sample was rewarmed, another aliquot of 100 μl was obtained and diluted for DLS measurement. The colloidal stability was studied for 1 month.

Effect of SPIONs and mCPA on primary cardiomyocyte viability in vitro

All of the following studies were performed using research protocols approved by the Institutional Animal Care and Use Committee

(IACUC) at the University of Florida. Primary cardiomyocytes from neonatal rat hearts were used in conjunction with Hoechst-PI assay to evaluate cell viability in the presence of CPA at different dilutions (25, 50, 75, and 100%), SPIONs at different concentrations (1, 2.5, 5, and 10 mg_{Fe}/ml), and mCPA at 5 mg_{Fe}/ml added gradually.

The Pierce Primary Cardiomyocyte Isolation Kit (Thermo Fisher Scientific) was used to isolate cardiomyocytes. Neonatal hearts were obtained from 2- to 3-day-old rats, within 30 min of the rat being euthanized. Cardiomyocytes were isolated and grown following the protocol provided in the isolation kit. Isolated cardiomyocytes were cultured in a 48-well plate at a density of 400,000 cells per well and allowed to grow for 3 days before performing the experiments.

All experiments were performed on ice in a cold room at 4°C to provide a temperature-controlled environment to minimize the toxicity of VS55. Cells were cooled for 10 min before beginning experiments. The solution was added and allowed to incubate for 21 min before removal (chosen based on typical times reported for CPA perfusion in organs in the literature) (*15*, *17*, *28*, *29*, *35*), incubated with Hoechst-PI for 5 min, and visualized under the microscope to assess VS55 and SPION toxicity. Hoechst stains all nuclei in blue, and PI stains all apoptotic/necrotic cells in red. The percentage of live cells was determined by calculating the difference between dead cells and the total number of cells.

Loading and removal of VS55 and mCPA solutions were performed in 3-min steps, gradually increasing the concentration as follows: 12.5% VS55 → 25% VS55 → 50% VS55 → 75% VS55 → 100% mCPA → 50% VS55 → 12.5% VS55 → medium. The cells were then incubated with Hoechst-PI for 5 min and visualized under the microscope. Viability was reported as the percentage of live to total cells counted from multiple images (more than 6000 cells per group), where $n = 3$ for each condition.

Evaluating whole-heart perfusion and removal with mCPA

Male Sprague-Dawley rats, 4 months old, were used for these studies. Initially, we evaluated perfusion of whole rat hearts with mCPA without vitrification or nanowarming. The approach was to (i) remove the heart, (ii) perfuse it with Custodiol HTK, (iii) perfuse it with mCPA, (iv) image it using MPI, (v) perfuse the heart with Custodiol HTK to remove the mCPA, and (vi) image the heart using MPI. To remove both the heart and lungs, the rat was first anesthetized and injected with 500 USP units of heparin to avoid clotting. Three minutes after administering heparin, the thoracic cavity was opened, and the following were ligated: inferior vena cava, superior vena cava, brachiocephalic trunk, left common carotid artery, and left subclavian artery. Once these were tied, the aorta and the inferior vena cava (below the tie) were cut, and the heart and lungs were removed and placed on ice. A plastic 26-gauge needle was tied in the aorta. A syringe filled with Custodiol HTK solution was attached to the needle, and the heart and lungs were perfused with 7 ml to remove the blood. The superior vena cava ligature was removed for the perfusate to exit. The syringe was replaced with a syringe filled with mCPA at 1 mg_{Fe}/ml, and 1.5 ml was injected. An additional 6 ml of Custodiol HTK solution was perfused as described above to perfuse out the particles.

We also evaluated perfusion of whole rat hearts with mCPA, followed by vitrification, nanowarming, and removal of the mCPA solution. Figure 5 illustrates the procedure taken for these experiments. The procedures to remove the heart and perfuse the organ were similar to those described above. The mCPA used in these experiments had a SPION concentration of 5 mg_{Fe}/ml, needed to achieve the required CWR of greater than 50°C/min. Once hearts were perfused with mCPA, a 20-gauge plastic needle was placed in the heart's center to insert the fiber-optic temperature probe used to monitor temperature during nanowarming. The heart was then submerged in the same mCPA solution used during perfusion and placed in a mechanical freezer to vitrify at a cooling rate of 15°C/min down to liquid nitrogen temperature of −196°C. Once the heart was vitrified, it was stored in a dewar filled with liquid nitrogen. One week later, the heart was removed from storage and nanowarmed using a field strength of 42.5 kA/m peak at a frequency of 278 kHz. Once the temperature inside the heart reached 0°C, the field was turned off and the mCPA was perfused out with Custodiol HTK solution.

A MOMENTUM imager (Magnetic Insight Inc.) was used to evaluate SPION perfusion through MPI. The hearts were imaged using 2D maximum intensity projection scans with a 12 cm × 6 cm field of view in isotropic mode at 5.9 T/m. A fiducial of known SPION concentration was imaged along with the heart for quantification. Images were analyzed using VivoQuant by selecting the heart and calculating the total signal observed in the region of interest, compared to the total signal obtained from the fiducial.

Hearts were fixed in formalin and sent to the UF College of Medicine Pathology Core for sectioning and staining. Transversal cross sections from the center and bottom of the rat hearts were obtained. Sections were 4 μm thick. Sections were stained using H&E and Prussian blue. H&E staining was used to assess heart structure, while Prussian blue was used as a complementary method to visualize particles in the heart.

SUPPLEMENTARY MATERIALS

Supplementary material for this article is available at http://advances.sciencemag.org/cgi/content/full/7/2/eabe3005/DC1

View/request a protocol for this paper from *Bio-protocol*.

REFERENCES AND NOTES

1. WHO-ONT, *Organ Donation and Transplantation Activities* (Global Observatory on Donation and Transplantation, 2016).
2. S. Giwa, J. K. Lewis, L. Alvarez, R. Langer, A. E. Roth, G. M. Church, J. F. Markmann, D. H. Sachs, A. Chandraker, J. A. Wertheim, M. Rothblatt, E. S. Boyden, E. Eidbo, W. P. A. Lee, B. Pomahac, G. Brandacher, D. M. Weinstock, G. Elliott, D. Nelson, J. P. Acker, K. Uygun, B. Schmalz, B. P. Weegman, A. Tocchio, G. M. Fahy, K. B. Storey, B. Rubinsky, J. Bischof, J. A. W. Elliott, T. K. Woodruff, G. J. Morris, U. Demirci, K. G. M. Brockbank, E. J. Woods, R. N. Ben, J. G. Baust, D. Gao, B. Fuller, Y. Rabin, D. C. Kravitz, M. J. Taylor, M. Toner, The promise of organ and tissue preservation to transform medicine. *Nat. Biotechnol.* **35**, 530–542 (2017).
3. J. K. Lewis, J. C. Bischof, I. Braslavsky, K. G. M. Brockbank, G. M. Fahy, B. J. Fuller, Y. Rabin, A. Tocchio, E. J. Woods, B. G. Wowk, J. P. Acker, S. Giwa, The grand challenges of organ banking: Proceedings from the first global summit on complex tissue cryopreservation. *Cryobiology* **72**, 169–182 (2016).
4. Health Resources and Services Administration's Division of Transplantation, The deceased donation process (2019); https://www.organdonor.gov/about/process/deceased-donation.html#expandcollapse.
5. P. E. Morrissey, M. L. Flynn, S. Lin, Medication noncompliance and its implications in transplant recipients. *Drugs* **67**, 1463–1481 (2007).
6. R. Yeter, M. Hübler, M. Pasic, R. Hetzer, C. Knosalla, Organ preservation with the organ care system. *Appl. Cardiopulm. Pathophysiol.* **15**, 207–212 (2011).
7. G. M. Fahy, B. Wowk, in *Cryopreservation and Freeze-Drying Protocols*, W. F. Wolkers, H. Oldenhof, Eds. (Springer New York, 2015), pp. 21–82.
8. C.-J. Zhou, D.-H. Wang, X.-X. Niu, X.-W. Kong, Y.-J. Li, J. Ren, H.-X. Zhou, A. Lu, Y.-F. Zhao, C.-G. Liang, High survival of mouse oocytes using an optimized vitrification protocol. *Sci. Rep.* **6**, 19465 (2016).
9. W. F. Rall, G. M. Fahy, Ice-free cryopreservation of mouse embryos at −196 °C by vitrification. *Nature* **313**, 573–575 (1985).

10. G. M. Fahy, B. Wowk, R. Pagotan, A. Chang, J. Phan, B. Thomson, L. Phan, Physical and biological aspects of renal vitrification. *Organogenesis* **5**, 167–175 (2009).
11. A. Arav, O. Friedman, Y. Natan, E. Gur, N. Shani, Rat hindlimb cryopreservation and transplantation: A step toward "organ banking". *Am. J. Transplant.* **17**, 2820–2828 (2017).
12. Z. Wang, B. He, Y. Duan, Y. Shen, L. Zhu, X. Zhu, Z. Zhu, Cryopreservation and replantation of amputated rat hind limbs. *Eur. J. Med. Res.* **19**, 28 (2014).
13. D. P. Eisenberg, J. C. Bischof, Y. Rabin, Thermomechanical stress in cryopreservation via vitrification with nanoparticle heating as a stress-moderating effect. *J. Biomech. Eng.* **138**, 011010 (2015).
14. M. L. Etheridge, Y. Xu, L. Rott, J. Choi, B. Glasmacher, J. C. Bischof, RF heating of magnetic nanoparticles improves the thawing of cryopreserved biomaterials. *Technology* **02**, 229–242 (2014).
15. M. J. Taylor, Y. C. Song, K. G. M. Brockbank, in *Life in the Frozen State*, B. J. Fuller, N. Lane, E. E. Benson, Eds. (CRC Press, 2004).
16. P. M. Mehl, Nucleation and crystal growth in a vitrification solution tested for organ cryopreservation by vitrification. *Cryobiology* **30**, 509–518 (1993).
17. N. Manuchehrabadi, Z. Gao, J. Zhang, H. L. Ring, Q. Shao, F. Liu, M. McDermott, A. Fok, Y. Rabin, K. G. M. Brockbank, M. Garwood, C. L. Haynes, J. C. Bischof, Improved tissue cryopreservation using inductive heating of magnetic nanoparticles. *Sci. Transl. Med.* **9**, eaah4586 (2017).
18. A. Chiu-Lam, C. Rinaldi, Nanoscale thermal phenomena in the vicinity of magnetic nanoparticles in alternating magnetic fields. *Adv. Funct. Mater.* **26**, 3933–3941 (2016).
19. J. Wang, G. Zhao, Z. Zhang, X. Xu, X. He, Magnetic induction heating of superparamagnetic nanoparticles during rewarming augments the recovery of hUCM-MSCs cryopreserved by vitrification. *Acta Biomater.* **33**, 264–274 (2016).
20. Z. Gao, H. L. Ring, A. Sharma, B. Namsrai, N. Tran, E. B. Finger, M. Garwood, C. L. Haynes, J. C. Bischof, Preparation of scalable silica-coated iron oxide nanoparticles for nanowarming. *Adv. Sci.* **7**, 1901624 (2020).
21. H. L. Ring, Z. Gao, A. Sharma, Z. Han, C. Lee, K. G. M. Brockbank, E. D. Greene, K. L. Helke, Z. Chen, L. H. Campbell, B. Weegman, M. Davis, M. Taylor, S. Giwa, G. M. Fahy, B. Wowk, R. Pagotan, J. C. Bischof, M. Garwood, Imaging the distribution of iron oxide nanoparticles in hypothermic perfused tissues. *Magn. Reson. Med.* **83**, 1750–1759 (2020).
22. W. Abdelwahed, G. Degobert, S. Stainmesse, H. Fessi, Freeze-drying of nanoparticles: Formulation, process and storage considerations. *Adv. Drug Deliv. Rev.* **58**, 1688–1713 (2006).
23. S. Deville, in *Freezing Colloids: Observations, Principles, Control, and Use: Applications in Materials Science, Life Science, Earth Science, Food Science, and Engineering*, S. Deville, Ed. (Springer International Publishing, 2017), pp. 91–170.
24. L. C. Wu, Y. Zhang, G. Steinberg, H. Qu, S. Huang, M. Cheng, T. Bliss, F. Du, J. Rao, G. Song, L. Pisani, T. Doyle, S. Conolly, K. Krishnan, G. Grant, M. Wintermark, A review of magnetic particle imaging and perspectives on neuroimaging. *Am. J. Neuroradiol.* **40**, 206–212 (2019).
25. E. Y. Yu, M. Bishop, B. Zheng, R. M. Ferguson, A. P. Khandhar, S. J. Kemp, K. M. Krishnan, P. W. Goodwill, S. M. Conolly, Magnetic particle imaging: A novel in vivo imaging platform for cancer detection. *Nano Lett.* **17**, 1648–1654 (2017).
26. R. E. Rosensweig, *Ferrohydrodynamics* (Dover Publications, 2014), 344 pp.
27. C. Barrera, A. P. Herrera, N. Bezares, E. Fachini, R. Olayo-Valles, J. P. Hinestroza, C. Rinaldi, Effect of poly(ethylene oxide)-silane graft molecular weight on the colloidal properties of iron oxide nanoparticles for biomedical applications. *J. Colloid Interface Sci.* **377**, 40–50 (2012).
28. M. J. Taylor, Y. C. Song, B. S. Kheirabadi, F. G. Lightfoot, K. G. M. Brockbank, Vitrification fulfills its promise as an approach to reducing freeze-induced injury in a multicellular tissue. *Adv. Heat Mass Transfer Biotechnol.* **363**, 93–102 (1999).
29. K. G. M. Brockbank, Z. Chen, E. D. Greene, L. H. Campbell, in *Cryopreservation and Freeze-Drying Protocols*, W. F. Wolkers, H. Oldenhof, Eds. (Springer New York, 2015), pp. 399–421.
30. Z. W. Tay, P. Chandrasekharan, A. Chiu-Lam, D. W. Hensley, R. Dhavalikar, X. Y. Zhou, E. Y. Yu, P. W. Goodwill, B. Zheng, C. Rinaldi, S. M. Conolly, Magnetic particle imaging-guided heating in vivo using gradient fields for arbitrary localization of magnetic hyperthermia therapy. *ACS Nano* **12**, 3699–3713 (2018).
31. Y. C. Song, B. S. Khirabadi, F. Lightfoot, K. G. M. Brockbank, M. J. Taylor, Vitreous cryopreservation maintains the function of vascular grafts. *Nat. Biotechnol.* **18**, 296–299 (2000).
32. H. Arami, A. Khandhar, D. Liggitt, K. M. Krishnan, In vivo delivery, pharmacokinetics, biodistribution and toxicity of iron oxide nanoparticles. *Chem. Soc. Rev.* **44**, 8576–8607 (2015).
33. F. Mérida, A. Chiu-Lam, A. C. Bohórquez, L. Maldonado-Camargo, M.-E. Pérez, L. Pericchi, M. Torres-Lugo, C. Rinaldi, Optimization of synthesis and peptization steps to obtain iron oxide nanoparticles with high energy dissipation rates. *J. Magn. Magn. Mater.* **394**, 361–371 (2015).
34. B. S. Lele, M. G. Kulkarni, Single step room temperature oxidation of poly(ethylene glycol) to poly(oxyethylene)-dicarboxylic acid. *J. Appl. Polym. Sci.* **70**, 883–890 (1998).
35. M. J. Taylor, B. P. Weegman, S. C. Baicu, S. E. Giwa, New approaches to cryopreservation of cells, tissues, and organs. *Transfus. Med. Hemother.* **46**, 197–215 (2019).

Acknowledgments

Funding: This work was supported by the University of Florida Vice President of Research Office. **Author contributions:** A.C.-L. and C.R. conceived and designed the experiments. C.J.P. and C.R. supervised the project and commented on the project. A.C.-L. synthesized and characterized the nanoparticles and cryopreservation agent solutions, assisted in animal experiments, and performed MPI studies. E.S. performed animal surgeries and whole-heart perfusions. A.C.-L. and C.R. analyzed the data and wrote the paper. All authors discussed the results and commented on the manuscript. **Competing interests:** C.R. and A.C.-L. are inventors on a pending patent related to this work filed by the University of Florida (no. 63/084,030, filed on 28 September 2020). The authors declare that they have no other competing interests. **Data and materials availability:** All data needed to evaluate the conclusions in the paper are present in the paper and/or the Supplementary Materials. Additional data related to this paper may be requested from the authors.

Submitted 12 August 2020
Accepted 19 November 2020
Published 8 January 2021
10.1126/sciadv.abe3005

Citation: A. Chiu-Lam, E. Staples, C. J. Pepine, C. Rinaldi, Perfusion, cryopreservation, and nanowarming of whole hearts using colloidally stable magnetic cryopreservation agent solutions. *Sci. Adv.* **7**, eabe3005 (2021).